



OPEN ACCESS

EDITED BY

Ernst Willingshofer,
Utrecht University, Netherlands

REVIEWED BY

Stephane Dominguez,
UMR5243 Géosciences Montpellier,
France
Gang Rao,
Southwest Petroleum University, China
Dan-Ping Yan,
China University of Geosciences, China

*CORRESPONDENCE

Victor Alania,
✉ victor.alania@tsu.ge
Onise E nukidze,
✉ onise.enukidze@tsu.ge

RECEIVED 28 March 2023

ACCEPTED 16 August 2023

PUBLISHED 30 August 2023

CITATION

Alania V, E nukidze O, Razmadze A,
Beridze T, Merkviladze D and
Shikhashvili T (2023), Interpretation and
analysis of seismic and analog modeling
data of triangle zone: a case study from
the frontal part of western Kura foreland
fold-and-thrust belt, Georgia.
Front. Earth Sci. 11:1195767.
doi: 10.3389/feart.2023.1195767

COPYRIGHT

© 2023 Alania, E nukidze, Razmadze,
Beridze, Merkviladze and Shikhashvili.
This is an open-access article distributed
under the terms of the [Creative
Commons Attribution License \(CC BY\)](https://creativecommons.org/licenses/by/4.0/).
The use, distribution or reproduction in
other forums is permitted, provided the
original author(s) and the copyright
owner(s) are credited and that the original
publication in this journal is cited, in
accordance with accepted academic
practice. No use, distribution or
reproduction is permitted which does not
comply with these terms.

Interpretation and analysis of seismic and analog modeling data of triangle zone: a case study from the frontal part of western Kura foreland fold-and-thrust belt, Georgia

Victor Alania^{1*}, Onise E nukidze^{1*}, Alexander Razmadze²,
Tamar Beridze², Demur Merkviladze³ and Tamar Shikhashvili³

¹Institute of Geophysics, I. Javakhashvili Tbilisi State University, Tbilisi, Georgia, ²A. Janelidze Institute of Geology, I. Javakhashvili Tbilisi State University, Tbilisi, Georgia, ³Faculty of Exact and Natural Sciences, I. Javakhashvili Tbilisi State University, Tbilisi, Georgia

2D seismic reflection profiles revealed the presence of a triangle zone at the frontal part of the western Kura foreland fold-and-thrust belt of the pro-wedge of the Greater Caucasus. To understand the triangle zone geometry, seismic interpretations should be substantiated by forward kinematic modeling, supported by analog experiments. This study presents a new structural model for the region by integrating field observations, well data, and seismic reflection data. East-West directed along-strike structural variation of the frontal thrust is observed on the interpreted seismic profiles which affected the fold geometry. The Bitsmendi breakthrough fault-propagation fold gradually transits into a wedge structure in the W-E direction and is represented by the triangle zone. The seismic profiles interpretation results completely match with analog models of similar triangle zones. The analysis of the experimental results helps us to further understand the kinematic evolution of natural systems and improve seismic interpretation. The triangle zone developed in the western part of the Bitsmendi breakthrough fault-propagation fold is related to double fault-bend fold structural wedges and is characterized by the presence of passive, and active wedges, and passive-backthrust and passive-forethrust.

KEYWORDS

Kura foreland fold-and-thrust belt, seismic profile, analog model, fault-propagation fold, fault-bend fold, wedge, triangle zone, fish-tail

1 Introduction

Triangle zones are common structures of many fold-and-thrust belts and are formed by linked, oppositely dipping thrusts that sole into one or more detachment levels, mainly near the deformation front (e.g., [Price, 1981](#); [McClay, 1992](#); [Jones, 1996](#); [Hagke and Malz, 2018](#); [Gil and Flinch, 2022](#)). The term triangle zone was first used by [Gordy et al. \(1977\)](#) in the Canadian Rocky Mountains. Generally, the triangle zones are interpreted to be associated with tectonic wedging and passive-roof duplex thrusts (e.g., [Banks and Warburton, 1986](#); [McClay, 1992](#); [Jones, 1996](#)). The triangle zones with several detachments involved are known

also as “fish-tail” or “zig-zag” structures. These structures form when the deeper detachment connects to the uppermost detachment by a ladder of thrust ramps of opposite vergence (e.g., Hagke and Malz, 2018; Gil and Flinch, 2022). According to Hagke and Malz (2018), triangle zones are classified into detachment-dominated (Type I) and ramp-dominated (Type II) triangle zones. Detachment-dominated triangle zones are related to a single ductile detachment and ramp-dominated triangle zones are linked to a secondary detachment and evolve due to bedding parallel slip at the upper ramp edge (Hagke and Malz, 2018). Geometric models of multiple types of triangle zones of fold-and-thrust belts are shown in Figure 1.

Analog and numerical models of triangle zones have been built to try to understand the geometry and kinematics of triangle zones related to one or several detachment levels (e.g., Pichot and Nalpas, 2009; Darnault et al., 2016; Granado et al., 2022).

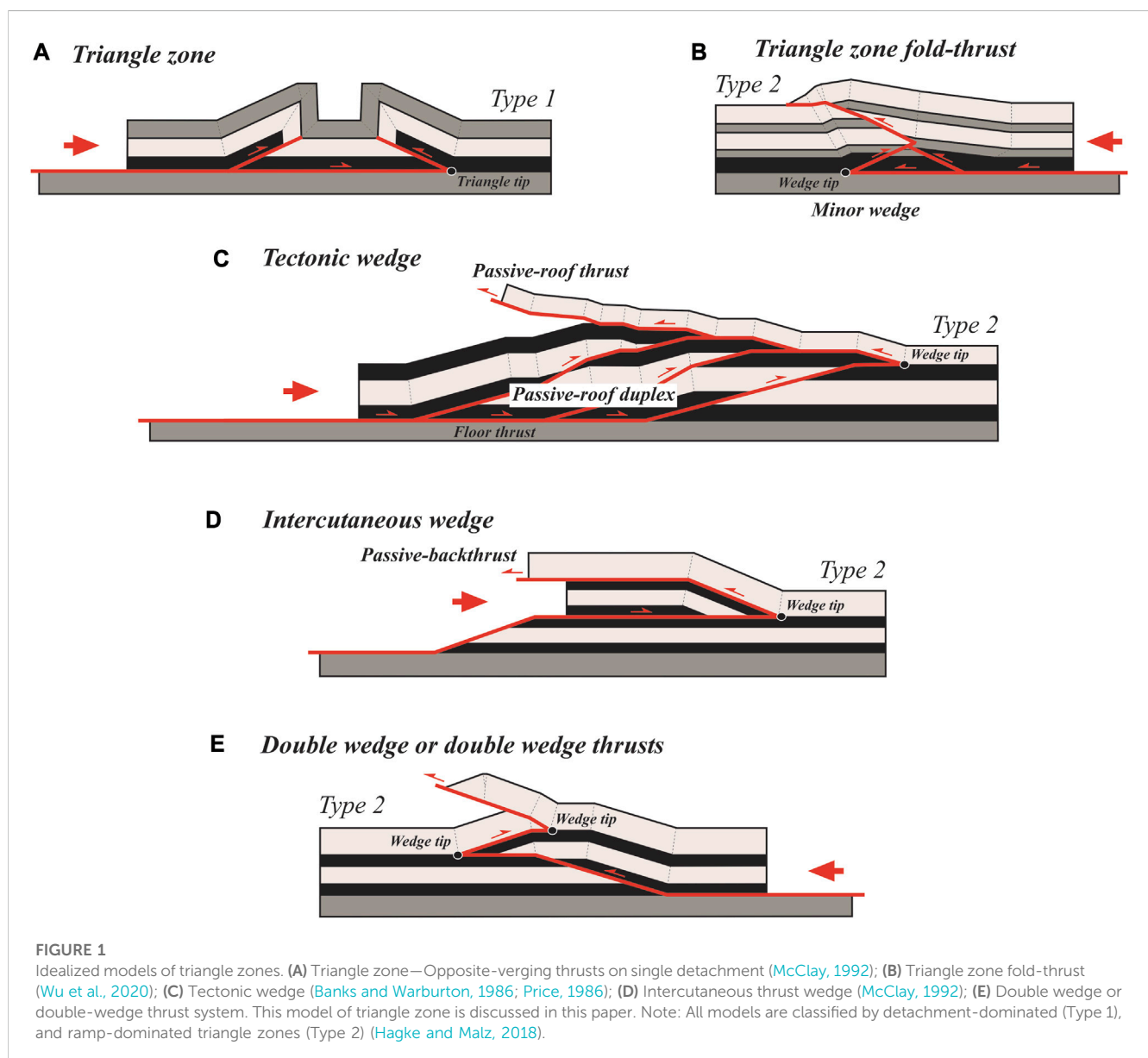
Presented in this study structural styles along the frontal part of the western Kura foreland fold-and-thrust belt (KFFTB), evidence

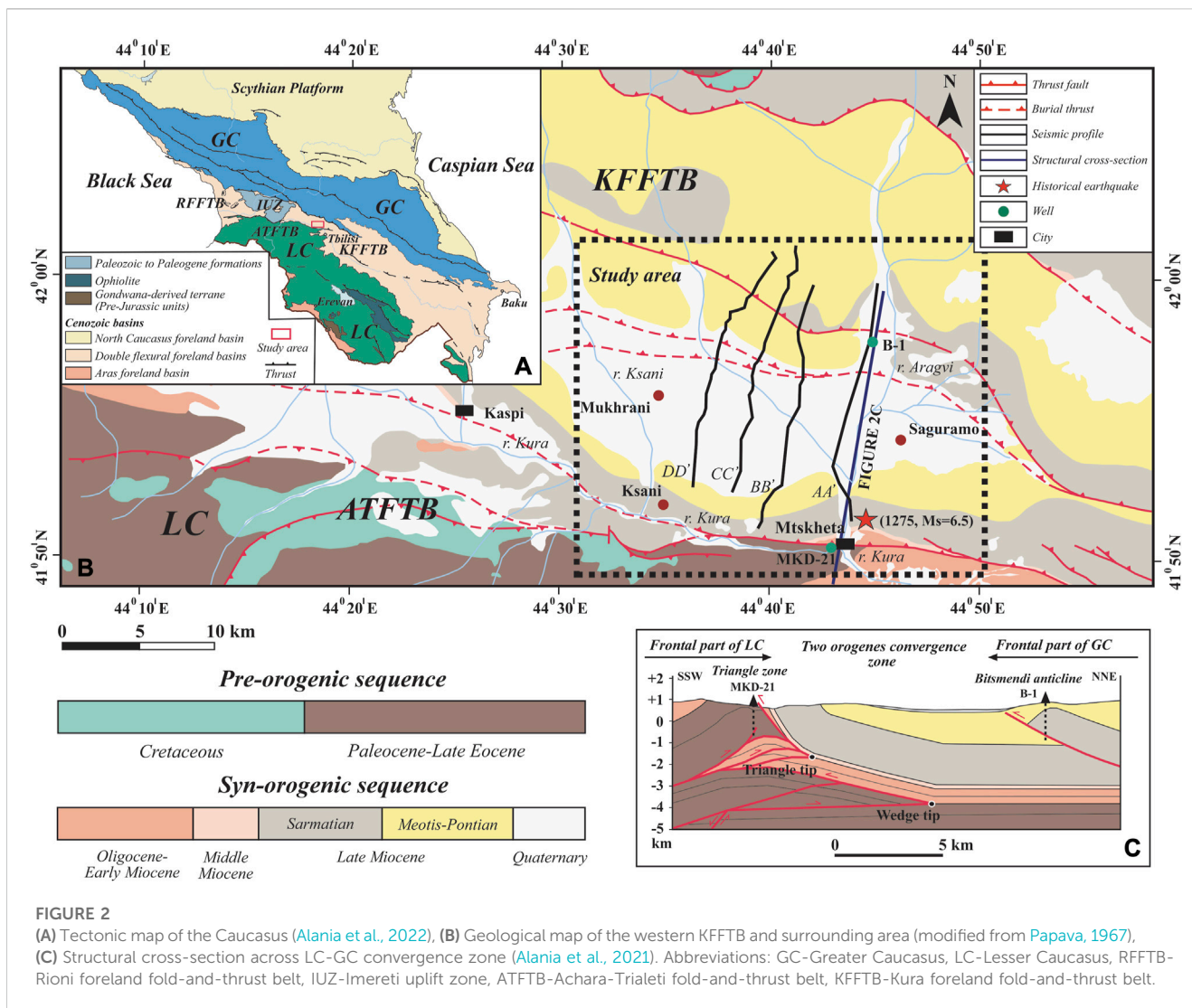
an evolution of triangle zone geometries like fish-tails. The formation of this triangle zone is related to a difference vergence of double wedge thrusts. In this study, we show the utility of this kinematic approach by matching seismic reflection profiles, and analog and forward kinematic models of triangle zone to gain further insight into the formation of these structures.

2 Geological setting

The KFFTB is located between the LC and the GC double wedge orogens (Figure 2A), which accommodates the crustal shortening due to far-field effects of the collision between the Arabian and Eurasian plates (e.g., Alania et al., 2021; Gusmeo et al., 2021).

Within our study area, the formation of the complex structure of the LC-GC convergence zone is governed by northward and southward-directed thrusting (e.g., Nemcok et al., 2013; Alania et al., 2021). Like the Pamir-Tien Shan convergence zones (e.g.,



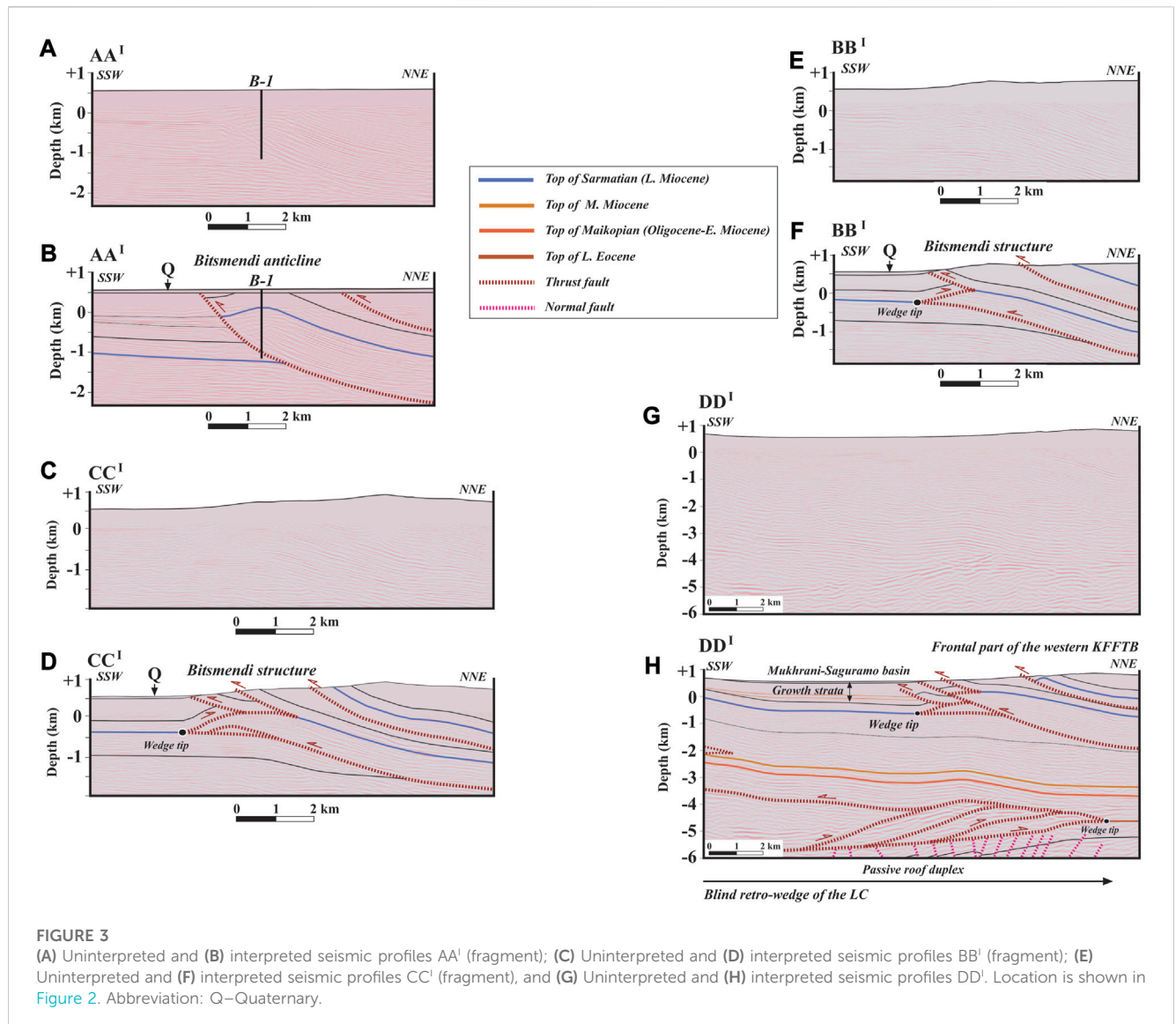


Fu et al., 2010), the LC-GC convergence zone is a unique example to understand ongoing intracontinental mountain building within the Arabia/Eurasia collision system. In the western part of the study area, the convergence zone of two orogens is introduced by frontal part of the LC retro-wedge and the GC pro-wedge (Figure 2B, C). The frontal part of the LC retro-wedge is represented by two different thrust systems: a shallow triangle zone and a lower structural wedge (e.g., Alania et al., 2021). The study area (Figure 2B) is situated in the frontal part of the western KFFTB in the pro-wedge of the central GC orogen. The western KFFTB is a south-vergent thrust system, most of which is associated with fault-related folds, and the thrust system involves about 2–3 km thick Miocene to Quaternary succession (e.g., Banks et al., 1997; Mosar et al., 2022).

The Kura foreland basin (KFB) developed mainly during the Oligocene-early Miocene through loading by the LC retro-wedge and the GC pro-wedge (Alania et al., 2021). On the basis of growth strata age and detrital apatite fission-track data, the onset of deformation in the KFB started in the Middle-Late Miocene (Alania et al., 2017; Gusmeo et al., 2021). Recent and historical

earthquakes indicate that the LC-GC convergence zone is tectonically active (e.g., Tsereteli et al., 2016).

The study area stratigraphy records the evolution from the extensional basins to the KFB of the Arabia-Eurasia collision zone (Alania et al., 2021). More than 7 km thick western KFB sedimentary infill consists of pre- and syn-orogenic sequences and is summarized in a tectonostratigraphic chart (Supplementary Figure S1). The pre-orogenic sequences consist of Jurassic-Late Eocene shallow and deep marine deposits. This series comprises mixed, siliciclastic-carbonate lithologies with an important mudstone level (Alania et al., 2021). The syn-orogenic sequences are composed of the foreland basin (Oligocene-Early Miocene) and syn-tectonic (Middle Miocene-Pleistocene) strata with the dominance of siliciclastic sequences (e.g., Alania et al., 2021). The thickness of the syn-orogenic sequence progressively increases northward and mainly comprises alternation of mudstones, sandstones, siltstones, and conglomerates of shallow marine and continental origin (Nemcok et al., 2013) (For further details see Supplementary Material).



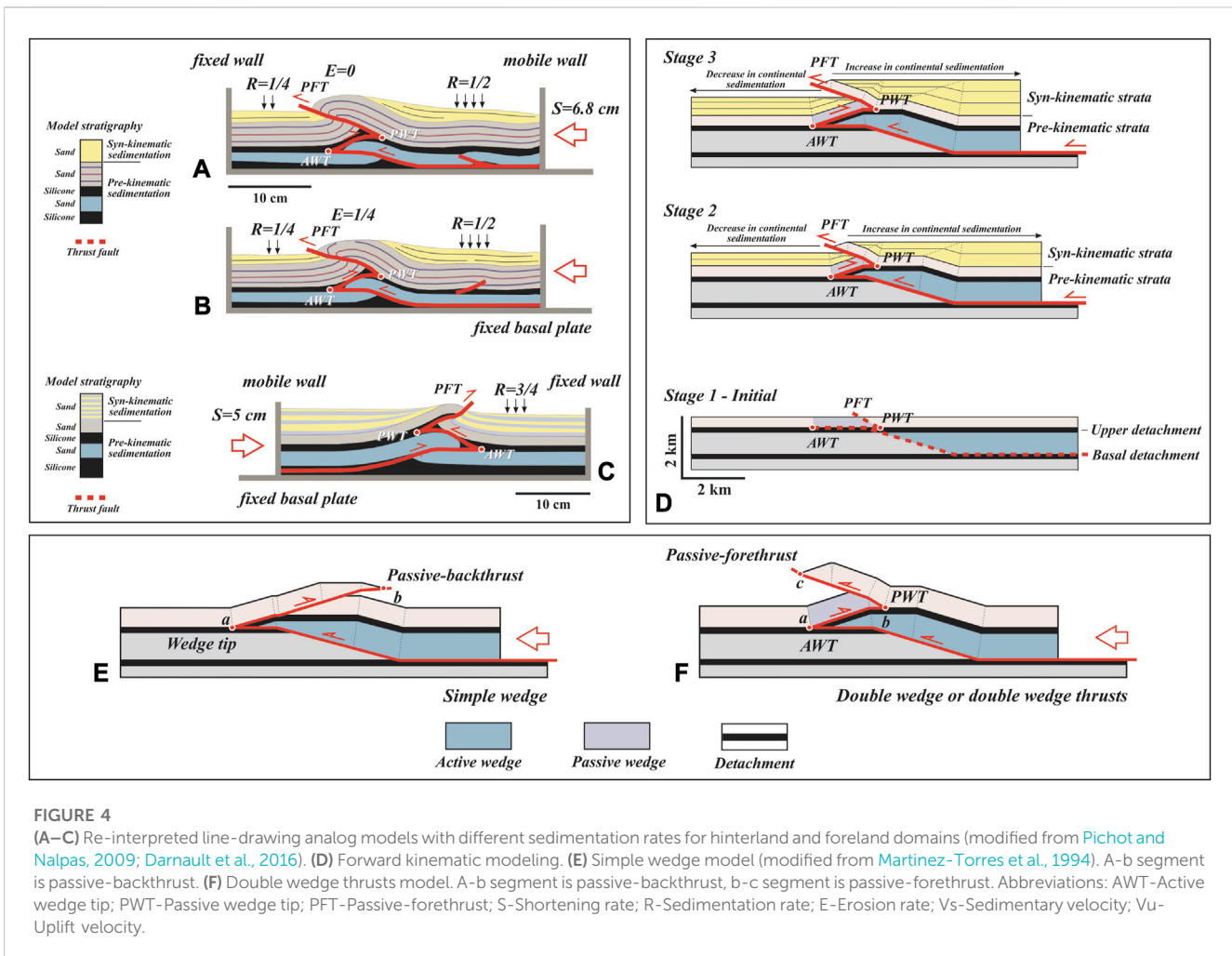
3 Data and methods

The surface geological information was obtained from a 1:100,000 geological map (Papava, 1967) of the study area (Figure 2B). To constrain the subsurface structure of the western KFFTB frontal part, we used four post-stack depth migrated 2D seismic profiles (Figure 3, Supplementary Figures S2–S4). Fault-related folding and wedge thrust theories (Suppe, 1983; Shaw et al., 2005) were used in the interpretation of 2D seismic profiles. For the interpretation of 2D seismic profiles, and building forward kinematic modeling was used the MOVE software. Fault-bend folding kinematic algorithms (cf. Suppe, 1983) were employed for the construction of the forward kinematic model (For further details see Supplementary Material). In the comparative analysis of triangle zone geometry and kinematics deduced from seismic profiles with analog modeling results we used published data (Pichot and Nalpas, 2009; Darnault et al., 2016) (Supplementary Figures S5, S6).

4 Results

4.1 2D seismic reflection profiles interpretation

All seismic lines (Line AA', BB', CC', and DD') are approximately perpendicular to the average strike of the main structures of the western KFFTB frontal part (Figure 2B). The seismic reflection profiles have revealed the geometry of triangle zone in the western KFFTB frontal part. The structural interpretation comprises four horizons (i.e., the top of Saratian—Late Miocene, Middle Miocene, Maikopian (Oligocene–Early Miocene), and Late Eocene), and south-vergent thrust faults (Figures 3B, D, F, H). Along Line AA' (Figure 3B), the frontal structure of the western KFFTB is represented by the Bitsmendi structure and is more compatible with a breakthrough fault-propagation fold (Suppe and Medwedeff, 1990).



Interpreted seismic profiles show that the Bitsmendi anticline was formed due to the movement along the frontal thrust fault of the western KFFTB and demonstrate significant along-strike variations in structural geometry. Observations of the Bitsmendi structure along Line BB', CC', and DD' (Figures 3D, F, H) are consistent with the geometric models of a structural wedge. In our case, the Bitsmendi breakthrough fault-propagation fold (Figure 3B) gradually transits into a wedge structure in the W-E direction and is represented by the triangle zone (Figures 3C, F, H). In the northern part of seismic profiles (Line BB', CC', and DD'), the Late Miocene syn-kinematic sediment thickness increase on the hinterland side, and the formation of fish-tail structure is related to two detachment levels (Figures 3C, F, H). The lower detachment is located in the lower part of Sarmatian mudstones (Late Miocene) and the upper detachment is developed between Sarmatian and Meotis-Pontian (Late Miocene) boundary (Supplementary Figure S1). On the seismic profile DD', the north-vergent passive-roof duplex, composed of Cretaceous-Late Eocene strata is developed below the LC-GC convergence zone and is represented by the part of blind retro-wedge of the LC. Below the north-vergent passive-roof duplex pre-growth units are complicated by normal faults (Figure 3H).

4.2 Comparison between seismic images and analog modeling

Many triangle zone structures were correlated between the analog model and the seismic images. For comparison with our seismic data, we used and re-interpreted published analog modeling data on triangle zones (Pichot and Nalpas, 2009; Darnault et al., 2016) which are fairly useful aids in kinematic evolution of frontal part of the western KFFTB of the GC pro-wedge. The results of these experiments were compared to natural examples from the sub-Andean thrust belt and are fairly similar to our study area (Figures 4A, B, C).

The main results provided by Pichot and Nalpas (2009) and Darnault et al. (2016) showed variations in the structural vergence, wedge geometry, the evolution of the deformation, and the decoupling of the lower and upper brittle structures in relation to the main parameters (shortening rate and mass transfer). These both experiments show: 1) a high sedimentation rate in the hinterland favors thrust development toward the foreland in the shallower parts, 2) a high sedimentation rate in the foreland involves a fault and fold vergence reversal, followed by a backthrusting of the shallower part (Supplementary Figures S5, S6 homogeneous sedimentation indicates that with the increase of sedimentation

velocity, the fault dip of the major upper brittle fault increases progressively (Supplementary Figure S6). (For further details of experiments see Supplementary Material).

4.3 Forward kinematic modeling

Using Move software and the geometric constraints provided by the seismic reflection data (Supplementary Figure S7), we generated a forward kinematic model (Figure 4D) of the triangle zone to test how effectively they could replicate the geometry of the Bitsmendi structure. The reflector characters of onlaps within the lower part of Meotian-Pontian (Late Miocene) units in the seismic profile BB', allowed the syn-kinematic (or growth) strata interpretation and have indicated that the formation of the triangle zone started at about 7 Ma (Supplementary Figure S7). Forward kinematic modeling shows that the triangle zone is developed in association with two detachment levels and the southward decrease of the syn-kinematic sedimentation produces a large variation in compressive structures (Figure 4D). The kinematic model of the sequential development of the triangle zone demonstrates that the formation of the Bitsmendi structure is related to the difference vergence of double wedge thrusts and is formed by the coeval activity of these thrusts that are linked at a wedge tip. As slip increases on the fault system, the wedge tip translates toward the foreland along the upper detachment level. The presence of north and south-vergent thrusts suggests that a component of slip on two detachments is accommodated by fault-bend fold structural wedging (Figure 4D).

5 Discussion

The transition from one type of fold into another (e.g., from the detachment into the fault-propagation fold or from the fault-propagation into the fault-bend fold) has been established in various fold-and-thrust belts (e.g., Hansman and Ring, 2018; Qiu et al., 2019; Jiang et al., 2020). If the fault tip of the fault-propagation fold occurs in the weaker sediments it may propagate along the bed as a detachment, forming a transported fault-propagation fold that subsequently deforms by fault-bend folding (Suppe and Medwedeff, 1990). The internal structure of the western KFFTB is laterally diversified by the rheology of the basal detachment in Late Miocene mudstones and the distribution of the syn-orogenic sediments. Obtained for the study area results fairly differ from previously existing models where the frontal part of the KFFTB was represented as a termination of the Bitsmendi fault-related fold (e.g., Banks et al., 1997; Mosar et al., 2022). The results presented here show that the frontal part of the western KFFTB along-strike Bitsmendi breakthrough fault-propagation fold was transitioned into fault-bend fold structural wedges and a triangle zone was developed in association with two detachment levels (Figure 3D, Supplementary Figure S7). This triangle zone is characterized as imbricated fault-bend fold structural wedges and divided by active and passive wedges (Figure 4F).

Based on the above-mentioned analog models' examples and forward kinematic modeling, the main parameters controlling the

structural evolution of triangle zones are the presence of i) detachment levels, ii) the amount and rate of shortening, and iii) the amount of syn-kinematic sedimentation. Interpreted line-drawing seismic profile BB' shows that together with high sedimentation rates the early Miocene sediments are duplicated by a south-vergent thrust, which conditions the increase in sediment thickness on the hinterland side (Supplementary Figure S7). The geometry of the structure is highly dependent on the sedimentation/uplift ratio. This implies that more fish-tail structures are developed when the syn-kinematic sedimentation rate is higher. Thus, the analog model's analysis allows us to compare them with the interpretation of seismic profiles. The seismic profiles interpretation results completely match with analog models of similar triangle zones (Figures 4A–C).

Using end-member modes of a wedge(s) (Martinez-Torres et al., 1994), the fish-tail like triangle zones which are controlled by wedge(s), can be divided into two types: i) simple wedge-dominated triangle zone (Figure 4E), and ii) double wedge-dominated triangle zone (Figure 4F). Simple-wedge triangle zone is composed of an active wedge and passive-backthrust. A double wedge-dominated triangle zone is represented by active, passive wedges, passive-backthrust, and passive-forethrust (Figures 4E, F).

The presence of detachment levels and a high sedimentation rate is a necessary but insufficient condition to produce such fish-tail structures. One example is the Tajik fold-and-thrust belt of the western foreland of the Pamir where theoretically all conditions for the formation of a triangle zone (high sedimentation rates and salt tectonic settings) existed (e.g., Gagala et al., 2020). Another example is the seismic profile across the northern Piedmont of the Tian-Shan range showing triangle zones in a single wedge tectonic setting in a similar geological situation (Qiu et al., 2019). Therefore, it is fair to ask why? In order to solve this problem, it is essential to conduct additional complex studies and hopefully in the future this question will be answered.

6 Conclusion

The western Kura foreland is a thin-skinned fold-and-thrust belt developed between two orogens, the LC-GC convergence zone. According to interpreted seismic profiles, the most common structures include fault-bend and fault-propagation folds, wedges, duplexes, and triangle zones. The structural styles presented in this study along the frontal part of the central GC pro-wedge, the Bitsmendi breakthrough fault-propagation fold gradually transits into a wedge structure in the EW direction and evidence evolution of triangle zone geometries related to a double wedge thrusts configuration as well as an evolution of triangle zone geometries. We have documented the dominant structural styles of the frontal part of the western KFFTB as the triangle zone and demonstrated how these are related to different vergence structural wedges involving two detachments. These structures form when the deeper detachment connects to the uppermost detachment by a ladder of wedges (passive and active) of opposite vergence. Application of these findings in the frontal part of the western KFFTB, as well as in the similar sub-Andean thrust belt could improve structural models and reduce uncertainty in structural interpretations.

Data availability statement

The original contributions presented in the study are included in the article/[Supplementary Material](#), further inquiries can be directed to the corresponding authors.

Author contributions

VA: Conceptualization; Data curation; Formal analysis; Investigation; Methodology; Project administration; Resources; Software; Validation; Visualization; Roles/Writing—original draft. OE: Conceptualization; Data curation; Funding acquisition; Investigation; Methodology; Resources; Supervision; Validation; Visualization; Writing—review and editing. AR: Conceptualization; Data curation; Formal analysis; Investigation; Methodology; Software; Validation; Visualization; Writing—review and editing. TB: Conceptualization; Data curation; Formal analysis; Investigation; Methodology; Software; Validation; Visualization; Writing—review and editing. DM: Conceptualization; Funding acquisition; Investigation; Methodology; Supervision; Validation; Visualization; Writing—review and editing. TS: Conceptualization; Data curation; Funding acquisition; Investigation; Methodology; Resources; Supervision; Validation; Visualization; Writing—review and editing. All authors contributed to the article and approved the submitted version.

Funding

The work was supported by the Shota Rustaveli National Science Foundation of Georgia (YS-21-612—Geometry and kinematic evolution of frontal part of the Eastern Achara-Trialeti fold-and-thrust belt).

References

- Alania, V., Beridze, T., Enukidze, O., Chagelishvili, R., Lebanidze, Z., Maqadze, D., et al. (2021) "The geometry of the two orogens convergence and collision zones in central Georgia: new data from seismic reflection profiles," in *Building knowledge for geohazard assessment and management in the Caucasus and other orogenic regions* Editor F. L. Bonali Editors (Springer, NATO Science for Peace and Security Series C: Environmental Security), Berlin, Germany, 73–88. doi:10.1007/978-94-024-2046-3_6
- Alania, V., Chabukiani, A., Chagelishvili, R., Enukidze, O., Gogrichiani, K., Razmadze, A., et al. (2017). Growth structures, piggy-back basins and growth strata of the Georgian part of the Kura foreland fold–thrust belt: implications for late alpine kinematic evolution. *Geol. Soc. Lond. Spec. Publ.* 428, 171–185. doi:10.1144/SP428.5
- Alania, V., Melikadze, G., Pace, P., Fõrizs, I., Beridze, T., Enukidze, O., et al. (2022). Deformation structural style of the Rioni foreland fold-and-thrust belt, Western Greater Caucasus: insight from the balanced cross-section. *Front. Earth Sci.* 10, 10968386. doi:10.3389/feart.2022.968386
- Banks, C. J., Robinson, A. G., and Williams, M. P. (1997). "Structure and regional tectonics of the Achara-Trialet fold belt and the adjacent Rioni and Kartli foreland basins, Republic of Georgia," in *Regional and Petroleum Geology of the black sea and surrounding region*. Editors A. G. Robinson, O. K. Tulsa, and United States (American Association of Petroleum Geologists Memoir), Washington, DC, USA, 68, 331–346. doi:10.1306/M68612C17
- Banks, C. J., and Warburton, J. (1986). 'Passive-roof' duplex geometry in the frontal structures of the Kirthar and Sulaiman mountain belts, Pakistan. *J. Struct. Geol.* 3, 229–237. doi:10.1016/0191-8141(86)90045-3
- Darnault, R., Callot, J-P., Ballard, J-F., Fraise, G., Mengus, J-M., and Ringenbach, J-C. (2016). Control of syntectonic erosion and sedimentation on kinematic evolution of a multidecollement fold and thrust zone: analogue modeling of folding in the southern subandean of Bolivia. *J. Struct. Geol.* 89, 30–43. doi:10.1016/j.jsg.2016.05.009
- Fu, B., Yoshiki, N., and Jianming, G. (2010). Slip partitioning in the northeast Pamir–Tian Shan convergence zone. *Tectonophysics* 483, 344–364. doi:10.1016/j.tecto.2009.11.003
- Gagala, L., Ratschbacher, L., Ringenbach, J. C., Kufner, S. K., Schurr, B., and Dedow, R. (2020). Tajik basin and southwestern tian-Shan, northwestern India-asia collision zone: 1. Structure, kinematics, and salt tectonics in the Tajik fold and thrust belt of the western foreland of the Pamir. *Tectonics* 39, e2019TC005871. doi:10.1029/2019TC005873
- Gil, W., and Flinch, J. F. (2022). Several types of triangle zones from the Subandean ranges of Peru: fish-tails, tectonic wedges and passive-roof duplexes. *Mar. Petr. Geol.* 146, 105968. doi:10.1016/j.marpetgeo.2022.105968
- Gordy, P., Frey, F., and Norris, D. K. (1977). Geological guide for the CSPG 1977 Waterton-Glacier Park field conference. *Can. Soc. Petrol. Geol. Calg.* 93.
- Granado, P., Ferrer, O., Santolaria, P., Muñoz, J., Roca, E., Gratacós, O., et al. (2022). "Analogue modeling as a tool to assist seismic structural interpretation in the Andean fold-and-thrust belt," in *Andean structural styles, A seismic atlas*. Editors G. Zamora and A. Mora (Elsevier), Amsterdam, Netherlands, 43–61. doi:10.1016/B978-0-323-85175-6.00003-1
- Gusmeo, T., Cavazza, C., Alania, V., Enukidze, O., Zattin, M., and Corrado, S. (2021). Structural inversion of back-arc basins-The Neogene Adjara-Trialeti fold-and-thrust belt (SW Georgia) as a far-field effect of the Arabia-Eurasia collision. *Tectonophysics* 803, 228702. doi:10.1016/j.tecto.2020.228702
- Hagke, C., and Malz, A. (2018). Triangle zones-geometry, kinematics, mechanics, and the need for appreciation of uncertainties. *Earth-Science Rev.* 177, 24–42. doi:10.1016/j.earscirev.2017.11.003
- Hansman, R. J., and Ring, U. (2018). Jabal Hafit anticline (UAE and Oman) formed by décollement folding followed by trishear fault-propagation folding. *J. Struct. Geol.* 117, 168–185. doi:10.1016/j.jsg.2018.09.014

Acknowledgments

We are fairly grateful to Georgian Oil and Gas Ltd. for providing the seismic profiles for our interpretation. We are thankful to Petroleum Expert (www.petex.com) for providing the academic license of MOVE software. Many thanks to the Guest Editor, EW, SD, and GR for their constructive comments and helpful suggestions.

Conflict of interest

The authors declare that the research was conducted in the absence of any commercial or financial relationships that could be construed as a potential conflict of interest.

Publisher's note

All claims expressed in this article are solely those of the authors and do not necessarily represent those of their affiliated organizations, or those of the publisher, the editors and the reviewers. Any product that may be evaluated in this article, or claim that may be made by its manufacturer, is not guaranteed or endorsed by the publisher.

Supplementary material

The Supplementary Material for this article can be found online at: <https://www.frontiersin.org/articles/10.3389/feart.2023.1195767/full#supplementary-material>

- Jiang, D., Wang, M., Song, G., Yan, B., and Feng, W. (2020). Transition from fault-propagation folds to fault-bend folds determined by along-strike variations of structural styles and fault displacement-distance relationships: the Sumatou anticline, Sichuan Basin, China. *J. Struct. Geol.* 131, 103951. doi:10.1016/j.jsg.2019.103951
- Jones, P. B. (1996). Triangle zone geometry, terminology and kinematics. *Bull. Can. Petrol. Geol.* 44, 139–152.
- Martinez-Torres, L. M., Ramon-Lluch, R., and Eguiluz, L. (1994). Tectonic wedges: geometry and kinematic interpretation. *J. Struct. Geol.* 16 (10), 1491–1494. doi:10.1016/0191-8141(94)90011-6
- McClay, K. R. (1992). “Glossary of thrust tectonics terms,” in *Thrust tectonics*. Editor K. R. McClay (Dordrecht, Netherlands: Springer), 419–433.
- Mosar, J., Mauvilly, J., Koiava, K., Gamkrelidze, I., Enna, N., Lavrishev, V., et al. (2022). Tectonics in the Greater Caucasus (Georgia–Russia): from an intracontinental rifted basin to a doubly verging fold-and-thrust belt. *Mar. Petr. Geol.* 140, 105630. doi:10.1016/j.marpetgeo.2022.105630
- Nemcok, M., Glonti, B., Yukler, A., and Marton, B. (2013). Development history of the foreland plate trapped between two converging orogens: kura Valley, Georgia, case study. *Geol. Soc. Lond. Spec. Publ.* 377, 159–188. doi:10.1144/SP377.9
- Papava, P. (1967). “Some question of eastern part of the Trialeti Ridge and perspective of oil-bearing of Cretaceous and Paleogene deposits,” in *Geology of the Georgian SSR*. Editor P. Gamkrelidze (Moscow: NEDRA), 188–204. (in Russian).
- Pichot, T., and Nalpas, T. (2009). Influence of synkinematic sedimentation in a thrust system with two decollement levels; analogue modelling. *Tectonophysics* 473, 466–475. doi:10.1016/j.tecto.2009.04.003
- Price, R. A. (1981). “The Cordilleran foreland thrust and fold belt in the southern Canadian Rocky Mountains,” in *Thrust and nappe tectonics*. Editors K. R. McClay and N. J. Price (Geological Society of London, Special Publications), London, UK, 9, 427–448.
- Qiu, J., Rao, G., Wang, X., Yang, D., and Xiao, L. (2019). Effects of fault slip distribution on the geometry and kinematics of the southern Junggar fold-and-thrust belt, northern Tian Shan. *Tectonophysics* 772, 228209. doi:10.1016/j.tecto.2019.228209
- Shaw, J. H., Connors, C. D., and Suppe, J. (2005). Seismic interpretation of contractional fault-related folds. *Aapg Studies In Geology*. American Association of Petroleum Geologists, Washington, DC, USA, 53. doi:10.1306/St531003
- Suppe, J. (1983). Geometry and kinematics of fault-bend folding. *Am. J. Sci.* 283, 684–721. doi:10.2475/ajs.283.7.684
- Suppe, J., and Medwedeff, D. A. (1990). Geometry and kinematics of fault-propagation folding. *Eclogae Geol. Helv.* 83, 409–454.
- Tsereteli, N., Tibaldi, A., Alania, V., Gventsadse, A., Enukidze, O., Varazanashvili, O., et al. (2016). Active tectonics of central-Western Caucasus, Georgia. *Tectonophysics* 691, 328–344. doi:10.1016/j.tecto.2016.10.025
- Wu, J., McClay, J., and De Vera, J. (2020). Growth of triangle zone fold-thrusts within the NW Borneo deep-water fold belt, offshore Sabah, southern South China Sea. *Geosphere* 16 (1), 329–356. doi:10.1130/GES02106.1